Biophysical Journal Volume 69 October 1995 1218–1229

The Secretory Granule Matrix-Electrolyte Interface: A Homologue of the p-n Rectifying Junction

Piotr E. Marszalek,* Vladislav S. Markin,‡ Toyoichi Tanaka,§ Haruma Kawaguchi,¶ and Julio M. Fernandez*
*Department of Physiology and Biophysics, Mayo Clinic, Rochester, MN 55905 USA; ‡Department of Cell Biology and Neuroscience, University of Texas Southwestern Medical Center, Dallas, TX 75235 USA; §Department of Physics and Center for Materials Science and Engineering, Massachusetts Institute of Technology, Cambridge, MA 02139 USA; and ¶Department of Applied Chemistry, Faculty of Science and Technology, Keio University, Yokohama, Japan

ABSTRACT When placed at the tip of a glass micropipette electrode the polymeric matrix of the secretory granule behaves like a diode. The measured current was 100-fold greater at negative potentials compared to positive potentials, and up to sixfold greater than that measured with the pipette alone. By manipulating the geometry of the electric field we show that these electrical properties result from focusing an electric field at the gel-electrolyte interface. We also show, by using pulsed-laser imaging with fluorescein as the ionic probe, that there is a rapid accumulation and depletion of ions at the gel-electrolyte interface. A voltage pulse of −9 V applied to the gel caused a severalfold increase in the fluorescence intensity within 5 ms. This correlated with an increase in the measured current (~1 μA). In contrast, within 5 ms of applying +9 V we recorded a decrease in the fluorescence intensity, which paralleled the twofold decrease in the measured current. This is similar to a p-n junction where an applied voltage causes the accumulation and depletion of charge carriers. Using synthetic gels (diameter 3–6 μm) with different charge characteristics we observed no rectification of the current with neutral gels and confirmed that rectification and amplification of the current were dependent on the fixed charge within a gel. In addition, we modeled the conduction at the gel-electrolyte interface using the Nernst-Planck electrodiffusion equation and accurately fitted the experimental current-voltage relationships.

This study provides some insight into how biological interfaces may function. For example, we suggest that neurotransmitter release during exocytosis could be regulated by voltage-induced accumulation and depletion of ions at the interface between the secretory granule and the fusion pore.

INTRODUCTION

The polymeric matrix of the giant secretory granules of beige mouse mast cells is highly responsive to electric fields when placed at the tip of a patch micropipette electrode (Nanavati and Fernandez, 1993). The secretory granule matrix displayed fast swelling and condensation in response to a voltage applied between the pipette's interior and the external medium. This behavior is indicative of "smart" synthetic polymer gels (DeRossi et al., 1991; Kajiwara and Ross-Murphy, 1992; Kishi and Osada, 1989; Kwon et al., 1991; Osada et al., 1992; Steinberg et al., 1966; Tanaka, 1981; Tanaka et al., 1982). The granule matrix also exhibited characteristics of a diode by rectifying the ionic currents. The polymeric matrix conducted currents 100-fold greater at negative rather than positive potentials. In addition, the current measured from the matrix-pipette assembly increased sixfold relative to that measured in the absence of the polymeric matrix; therefore the matrix not only rectifies but also amplifies the pipette current (Nanavati and Fernandez, 1993).

Rectification requires asymmetry. In the case of a junction between two semiconductors (e.g., p-n junction), this asymmetry results from different majority carriers in each material. This arrangement sets up a potential barrier, preventing the flow of current across the junction (Kittel, 1976). When an externally applied voltage decreases this barrier (junction potential) the charges readily diffuse across the junction. This results in the accumulation of charges in the transition region between both semiconductors and facilitates the flow of current. The reverse case of increasing the potential barrier depletes the transition region of the charge carriers, inhibiting the flow of current. We show that a similar mechanism of voltage-induced accumulation and depletion of charge carriers operates at the polymeric matrix-electrolyte interface. The polymeric matrix of the secretory granule is a gel, and because it is composed of negatively charged heparin sulfate proteoglycan it has a high density of fixed charges (Fernandez et al., 1991). Thus by Donnan exclusion (Helfferich, 1962; Tam and Verdugo, 1981) the concentration of mobile co-ions in the secretory granule gel is much lower than the counter-ion concentration, and the current flowing through this gel is carried mainly by counter-ions. This contrasts with electrolyte solutions in which both ionic species carry the current. Therefore, the interface between the secretory granule gel and an electrolytic solution resembles a junction between two semiconductors.

In this paper we employ this analogy to examine and explain the electrical properties of the secretory granule gel (Nanavati and Fernandez, 1993). In addition to electrical measurements we use pulsed-laser imaging (Monck et al.,

Received for publication 27 April 1995 and in final form 23 June 1995.
Address reprint requests to Dr. Julio M. Fernandez, Department of Physiology/Biophysics, Mayo Clinic and Foundation, 1-159 Medical Sciences Building, Rochester, MN 55905 USA. Tel.: 507-284-0423; Fax: 507-284-0521; E-mail: fernandez.julio@mayo.edu.

0006-3495/95/10/1218/12 $2.00

1994) to monitor the distribution of ions at the gel-electrolyte interface. To demonstrate the role of the fixed charges in the rectification and amplification of the current we conduct identical experiments using synthetic (charged and neutral) gels. By placing a gel at the tip of a micropipette we were able to study the conduction at a *single* gel-electrolyte interface. This was possible because the geometry of the pipette focuses the electric field at the interface between the gel and the solution confined within the pipette. This interface controls the conductance of the gel-pipette assembly.

We compare our experimental measurements with a theoretical model and suggest some biological implications.

MATERIALS AND METHODS

Hydrogels

Isolated giant secretory granules were prepared by sonication of purified beige (bg^j/bg^j) mouse mast cells obtained by peritoneal lavage (Nanavati and Fernandez, 1993; Monck et al., 1991). The anionic heparin proteoglycan hydrogel (1–5 μm) is a core of the secretory granule. The synthetic amphoteric microspheres (~6 μm) were prepared by copolymerization of methacrylic acid and *p*-nitrophenyl acrylate, with methylenebisacrylamide as a cross-linker and 2,2′-azobisisobutylonitrile as an initiator (Kashiwabara et al., 1993). The reaction was carried out in ethanol (10 mM methacrylic acid/10 mM *p*-nitrophenyl acrylate/5 mM MBA/35 g ethanol/0.75 g 2,2′-azobisisobutylonitrile) at 60°C for 22 h under nitrogen. The particles were then modified for 48 h at room temperature in the presence of ethylenediamine (particle/ethylenediamine = 1 eq/100 eq). The hydrogel is amphoteric, with a pK of ~4 as determined by electrophoresis. In some experiments we also used neutral gel microspheres (5–50 μm in diameter) that were composed of *N*-isopropylacrylamide and methylenebisacrylamide.

Electrical measurements

The experimental arrangement is outlined in Fig. 1. A hydrogel particle was placed at the tip of a glass micropipette (P_1 in Fig. 1, *A* and *B*). The geometry of the electric field applied to the hydrogel particle was controlled by varying the distance between the two pipettes (P_1 and P_2). This distance was controlled by two micromanipulators. The pipettes and bathing medium were filled with identical saline solutions, and unless otherwise specified the solutions contained histamine dichloride (1 to 100 mM) buffered with citric acid or HEPES.

The electrical arrangement is shown in Fig. 1 *B*. Silver/silver chloride electrodes were inserted in the pipettes. The voltage supplied to the pipettes was controlled by the current-voltage converter, which had a gain of 1.212 mV nA^{-1}. We used an IDA 15125 interface (INDEC Systems, Sunnyvale, CA) for applying command voltages and for data acquisition, operating from a Gateway 2000 computer (Gateway Co., Sioux City, SD).

Pulsed laser imaging

Fluorescein (Sigma Chemical Co.), a fluorescent anion was used as the ionic probe. It was added to the pipette solution at small concentrations (100–300 μM). The imaging system (Monck et al., 1994) consisted of an inverted epifluorescence microscope (model IM-35, Carl Zeiss, Oberkochen, Germany) coupled to a high-intensity pulsed coaxial flash lamp dye laser (LuminX Model LS-1400, Phase-R Corporation, New Durham, NH), which provided short (350 ns) pulses of illumination. Attached to the microscope was a cooled charge-coupled device camera (model C200, Photometrics Ltd., Tuscon, AZ). A microcomputer (Compaq Desk pro 386/25, Compaq Computer Corp., Houston, TX) controlled image acquisition and image processing. An IDA interface was used for data acquisition and synchronization of the laser with the current measurements. The lasing dye was Coumarin 480. The typical experimental procedure involved acquiring an image of the gel when no voltage pulse (control) was applied and then capturing an image of the gel during a voltage pulse (stimulus). The fractional change in fluorescence was calculated from the ratio of the stimulus image divided by the control image. This procedure was repeated several times at different points along the voltage pulse. This allowed us to characterize the time dependence of the redistribution of ions. Images were filtered digitally using an inverse filter designed to remove out-of-focus light (Monck et al., 1992).

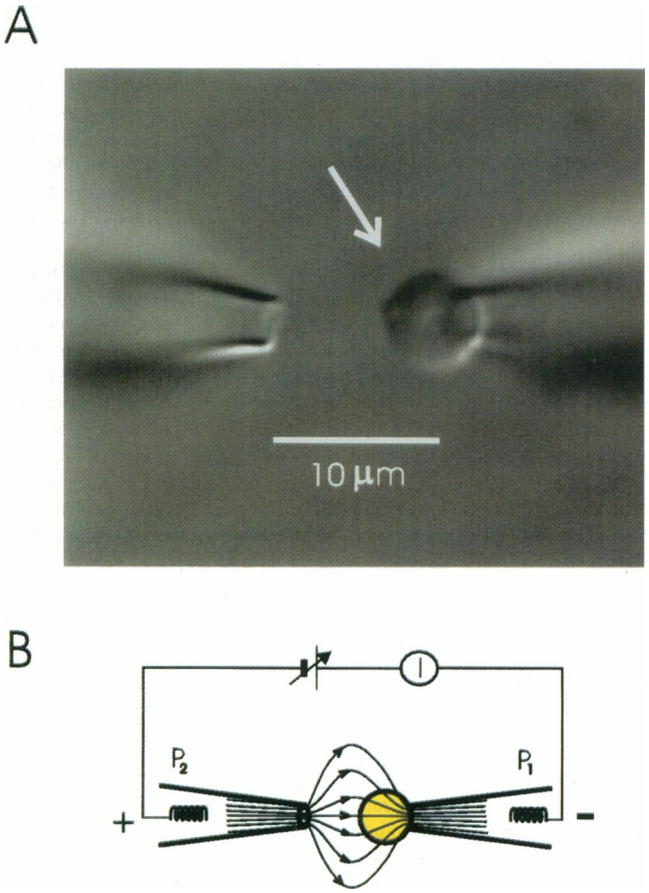

FIGURE 1 Experimental arrangement used to apply an electric field of variable geometry to a micron-sized hydrogel microparticle. (*A*) The figure shows a synthetic hydrogel microparticle (~6 μm in diameter; arrow) placed at the tip of a glass micropipette (P_1; tip size 0.5–3 μm). A second pipette (P_2) is placed at a variable distance from P_1. (*B*) A voltage difference applied between the two pipettes establishes an electric field across the gel interfaces. The geometry of the electric field across the external surface was changed by varying the distance between the pipettes.

THEORETICAL MODEL

Description of the gel-electrolyte interface

The interface between a charged gel and an electrolyte solution resembles a junction between two different semiconductors. There is a Donnan potential at the gel-electrolyte interface that is similar to the semiconductors' junction potential. This Donnan potential reduces the diffusion of ions across the interface. When the external voltage applied to the gel-electrolyte interface has a polarity opposite that of the Donnan potential the mobile co-ions of the electrolyte are pushed toward the interface, but

because only a limited number of them can penetrate into the gel (Donnan exclusion) they accumulate at this interface. Electroneutrality requires that counter-ions also accumulate at the gel-electrolyte interface. Because the ionic concentration at this interface is high, conditions are favorable for the flow of current, most of which is carried by the counter-ions. When the polarity of the external voltage is the same as the Donnan potential, the mobile co-ions are pulled into the bulk electrolyte. Because the fixed negative charges cannot diffuse into the bulk electrolyte the interface is quickly depleted of both the mobile co-ions and counter-ions. The conditions then become unfavorable for the flow of current.

When a charged gel is placed at the tip of a glass micropipette, two interfaces are established: one between the gel and the medium confined in the pipette (internal gel-electrolyte interface) and the other between the gel and the bathing medium (external gel-electrolyte interface, Fig. 1 *B*). Although we have two interfaces the micropipette focuses the electric field at the internal gel-electrolyte interface. Most of the voltage drop occurs at this interface, with greater changes in ion concentrations taking place there. In contrast, the field is dispersed at the external gel-electrolyte interface, which receives a small fraction of the applied voltage and experiences very limited changes in the ion concentration. Therefore by placing the microgel at the tip of a glass micropipette we are able to examine one rectifying junction.

Current-voltage relationship for the gel-pipette assembly

We now outline the principal equations of our theoretical model valid at steady state. A more complete derivation of the model is given in the Appendix. From the Nernst-Planck electrodiffusion equation (Bockris and Reddy, 1977) we derive the current-voltage relationship for a gel attached to the tip of a pipette and immersed in a binary electrolyte.

An expression for the electrolyte concentration at the internal gel-electrolyte interface $c(x_i)$ in terms of the voltage applied to the solution in the pipette is

$$c(x_i) = c^0 \exp\left[\frac{z_{acc}F(\varphi_p - \varphi(x_i))}{RT}\right] \quad (1)$$

where c^0 is the bulk concentration of electrolyte, φ_p is the voltage applied to the solution in the pipette, $\varphi(x_i)$ is the potential at the internal gel-electrolyte interface, F is the Faraday constant, R is the gas constant, T is the absolute temperature, and z_{acc} is the accumulation charge, which is defined as

$$z_{acc} = \frac{\alpha_+ z_- D_- + \alpha_- z_+ D_+}{D_- \alpha_+ + D_+ \alpha_-} \quad (2)$$

where α_+ and α_- are the transference numbers; D_+ and D_- are the diffusion coefficients; and z_+ and z_- are the charge numbers for cations (+) and anions (−).

It is obvious from Eq. 1 that when $z_{acc} = 0$ the concentration in the pipette is the same as in the bulk. This occurs either when there is no gel attached or the gel is uncharged. If most of the current is carried by the counter-ions, z_{acc} will approach the charge number of the impermeable co-ion, i.e., $z_{acc} \rightarrow z_{co\text{-}ion}$. In addition, Eq. 1 shows that a negatively charged gel ($z_{acc} < 0$) will increase the electrolyte concentration at the gel-electrolyte interface at negative potentials and decrease the electrolyte concentration at positive potentials. The opposite effect will occur with a positively charged gel ($z_{acc} > 0$).

An expression of the current (I) as a function of the applied potential is given by

$$I = -\frac{RT}{z_{acc}F}\frac{1}{R_p^0}\left\{1 - \exp\left[\frac{z_{acc}F(\varphi_p - \varphi(x_i))}{RT}\right]\right\} \quad (3)$$

where R_p^0 is the pipette resistance in the absence of the gel.

Because the voltage drop across the external solution is negligible (see Appendix), $\varphi(x_i)$ is the potential drop across the gel particle, $\varphi(x_i) = R_g I$, where R_g is the particle resistance. Therefore Eq. 3 can be simplified to

$$\varphi_p = R_g I + \frac{RT}{z_{acc}F}\ln\left[1 + \frac{z_{acc}FR_p^0}{RT} I\right] \quad (4)$$

It is apparent from Eq. 3 that a negatively charged gel ($z_{acc} < 0$) will cause the current to saturate at positive potentials. At the limit $\varphi_p \rightarrow +\infty$ the expression for the saturation current (I_{rev}) becomes

$$I_{rev} = -\frac{RT}{z_{acc}F}\frac{1}{R_p^0} \quad (5)$$

and I_{rev} is proportional to the initial (without gel) conductance of the pipette. Substituting Eq. 5 into Eq. 4, the current-voltage relationship for the gel-pipette assembly can be written as

$$\varphi_p = R_g I - I_{rev}R_p^0 \ln\left(1 - \frac{I}{I_{rev}}\right) \quad (6)$$

Combining Eqs. 1, 3, and 5 leads to a convenient formula expressing the electrolyte concentration as a function of the current:

$$\frac{c}{c_0} = 1 - \frac{I}{I_{rev}} \quad (7)$$

RESULTS AND DISCUSSION

Current-voltage relationships

Outlined in Fig. 2 *A* is the I-V curve obtained in the absence of a gel. The relationship is linear; this indicates that there are no detectable nonlinearities: within the electrodes, at the liquid-liquid interfaces, and/or arising from strong electric fields (Onsager, 1934). In contrast, when a gel was attached to one of the pipettes (P_1) diode-like rectification was observed (Fig. 2 *B*). Current flowed from pipette P_2 to P_1 when P_1 was held at a lower potential than P_2, but very little current flowed from pipette P_1 to P_2 when P_1 was held at more positive potential than P_2. When the gel was transferred from pipette P_1 to P_2 the current flowed in the opposite direction (Fig. 2 *E*). This shows that the hydrogel is able to conduct current in either direction and suggests that rectification is not an intrinsic property of the gel.

When pipette 2 (P_2) was brought closer to the gel (~1 μm, Fig. 2 *C*) the current still flowed from P_2 to P_1, but reached a saturation current of ~ −100 nA at ~ −2 V. Bringing the pipette into contact with the gel caused the current to almost disappear at both potentials (Fig. 2 *D*). These observations (Fig. 2 *B–D*) can be explained in terms of the differences in the electric field distribution among the experiments outlined in Fig. 2 *B–D*. In Fig. 2 *B*, when the pipettes are at a considerable distance apart (>100 μm), the electric field is highly focused at the internal gel-electrolyte interface and dispersed at the external gel-electrolyte interface. Because the voltage drop is much larger at the internal gel-electrolyte interface it controls the flow of current and determines the current-voltage relationship. In Fig. 2 *C* and *D* the pipette was brought closer to the exposed gel surface

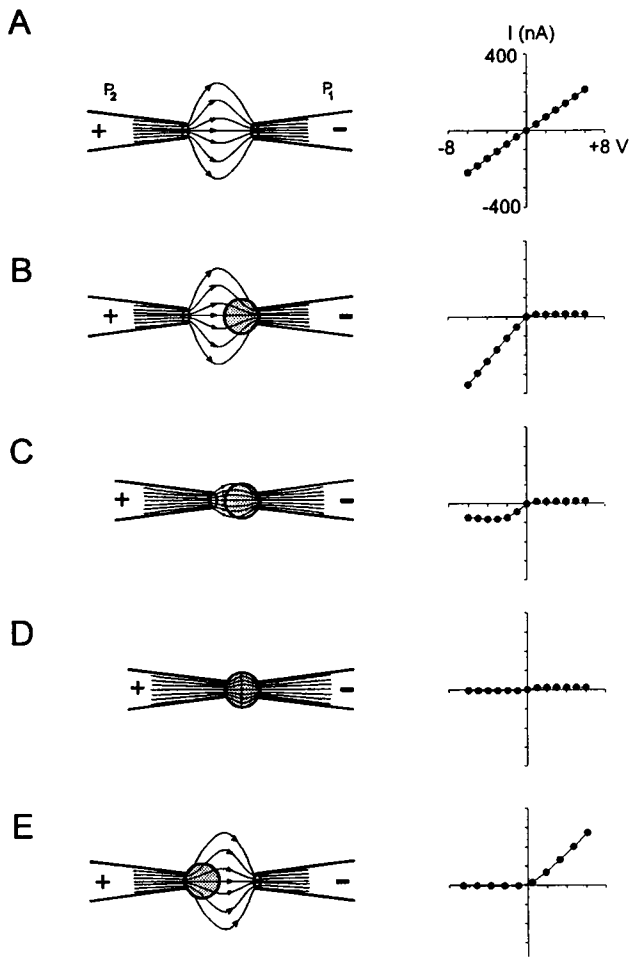

FIGURE 2 Effect of the geometry of the applied electric field on the current-voltage relationship of a hydrogel microparticle placed at the tip of a glass pipette. In this series of experiments natural anionic heparin proteoglycan hydrogels were used. (*A*) No gel present. (*B*) A hydrogel microparticle is placed at the tip of pipette P_1 with the second pipette P_2 placed at a considerable distance (> 100 μm) from the gel. (*C*) Pipette P_2 was placed ~1 μm away from the external surface of the hydrogel. (*D*) Pipette P_2 touches the external gel surface. (*E*) The hydrogel microparticle is pushed out of the tip of P_1 (hydrostatically by applying pressure to the interior of the pipette) and transferred to pipette P_2 (by suction). Pipette P_1 was placed a considerable distance (> 100 μm) from the gel. The medium filling the pipettes and the bath was 10 mM histamine dihydrochloride buffered at pH 3.6 with 0.5 mM citric acid.

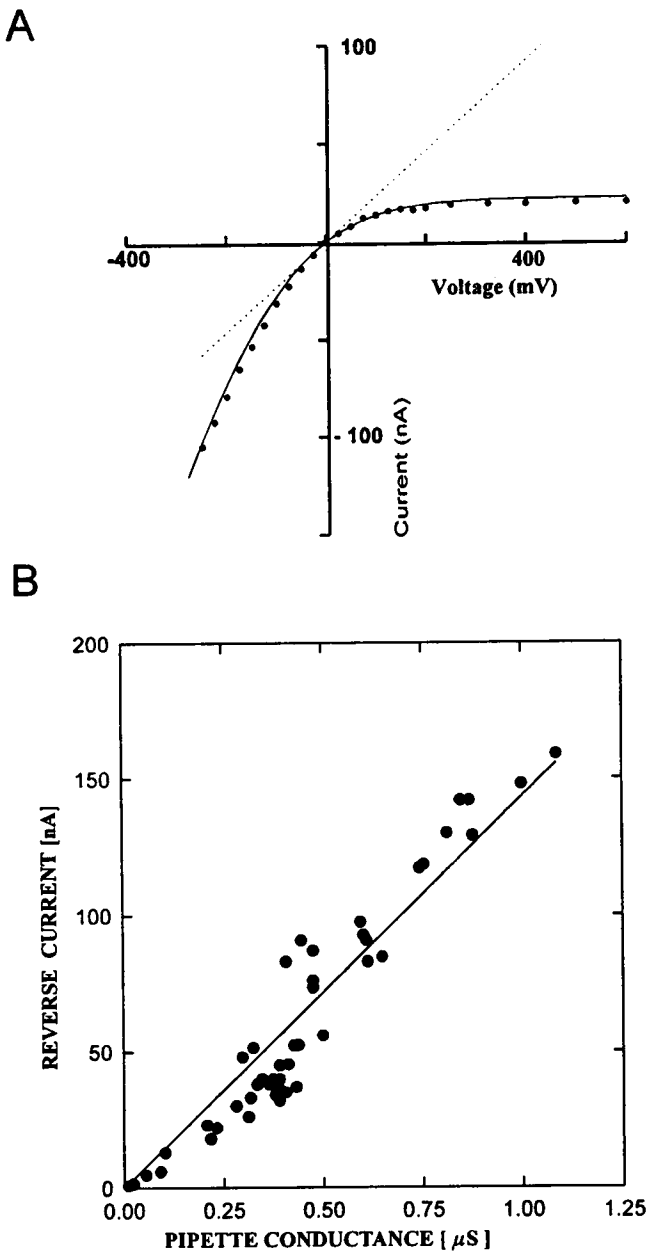

FIGURE 3 (*A*) Experimental (●) and theoretical (solid line) current-voltage relationships for the secretory granule gel. Dotted line represents the current-voltage relationship of the pipette in the absence of the gel particle (control current). The solid line represents the fit of Eq. 4 to the experimental data. Solution: 25 mM histamine dihydrochloride, 5 mM citric acid, pH = 3.5. (*B*) Dependence of the reverse (saturation) current, I_{rev}, of the natural hydrogel on the pipette conductance $(R_p^0)^{-1}$. The pipette conductance was changed by altering the size of the pipette opening, and by varying the concentration of the electrolyte (histamine dihydrochloride) from 1 to 100 mM. The solid line represents a linear regression of the data; the accumulation charge, z_{acc}, is determined from the slope $-RT/z_{acc}F$ of the line (Eq. 5).

(~1 μm away in Fig. 2 *C*) the electric field is focused not only at the internal gel-electrolyte interface but also at the external gel-electrolyte interface. The latter now experiences a significant voltage drop, which causes the current to dramatically decrease. These two interfaces behave like two oppositely polarized diodes that cannot conduct current when connected in series. These experiments not only show that the rectification originates at the internal gel-electrolyte interface, but also reveal that the external gel-electrolyte interface has minimal influence on the current-voltage relationship unless it experiences a significant voltage drop (cf. Fig. 2 *B* and *D* and see Appendix).

Outlined in Fig. 3 *A* is the current-voltage relationship observed at higher resolution. At positive potentials the current is not null but saturates at a magnitude of ~20 nA at ~200 mV. We fitted the data to Eq. 4 and determined the

gel resistance (R_g) and the accumulation charge (z_{acc}) for this granule to be 0.84 MΩ and −0.3, respectively. From the accumulation charge, we estimate transference numbers for cations and anions of $\alpha_+ = 0.77$ and $\alpha_- = 0.23$, respectively. This calculation assumes the diffusion coefficients of cations and anions are equal, but it is unknown if this assumption is valid for the gel. Shown in Fig. 3 *B* is the plot of the reverse current, I_{rev}, against pipette conductance $[(R_p^0)^{-1}$, i.e., the conductance of the pipette determined in the absence of the gel]. This relationship is approximately linear and once again there is a reasonable fit between experimental data and theory. From the slope and Eq. 5 we calculate an average value for the accumulation charge(z_{acc}) of −0.2; this is close to the value obtained from Fig. 3 *A*.

The accumulation of ions at the gel-electrolyte interface is demonstrated by the experimental result outlined in Fig. 4. In this set-up the natural gel was immersed in saline solution and allowed to adhere to a glass slide. The pipette tip was then brought toward the immobilized gel until a contact formed. A voltage pulse (negative, time ~8 s) was applied to the pipette-gel assembly, and the current was monitored before and after the contact between the gel and the pipette was broken. This contact was destroyed by quickly moving the pipette ~100 μm away from the gel. At this separation the gel no longer affects the current. During this manipulation, which took the equivalent of 6 video frames (i.e.,~ 200 ms), the current did not decrease immediately, but it took ~ 3.5 s to reach the same magnitude as the control. (In the control, the current was measured with a pipette immersed in the bathing medium with no gel attached throughout the whole voltage pulse, and the movement of the pipette in this case did not cause any change in the current.) Because the pipette current was significantly elevated even after the contact between the gel and the pipette was disabled this indicates that ions (i) accumulate in the pipette at the internal gel-electrolyte interface, increasing the pipette's conductance, and (ii) take a finite time to diffuse.

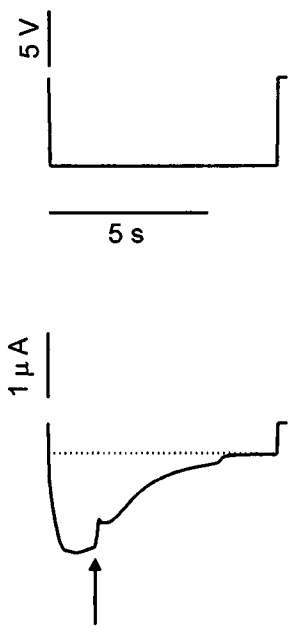

FIGURE 4 Time course of the pipette current in the presence of the natural gel and immediately after the pipette-gel contact was disabled. A voltage pulse (−8 V, top) was applied to the pipette-gel assembly. At the moment indicated by the arrow the pipette was quickly moved away from the immobilized gel, while the current was continuously recorded. The dotted line represents the control current measured under the same voltage conditions, i.e., no gel present throughout the experiment. See text for further details.

Synthetic gels

To verify if amplification and rectification of the current are unique properties of the negatively charged natural polymers or a general feature of charged gels when they are attached to a micropipette, we conducted a series of experiments with synthetic amphoteric gels (see Materials and Methods). Outlined in Fig. 5 is a series of current-voltage relationships obtained when a synthetic gel was attached to the pipette tip (Fig. 1). At pH 7.0 the synthetic gel has a net negative charge (Fig. 5 *A*, left), at negative potentials the gel

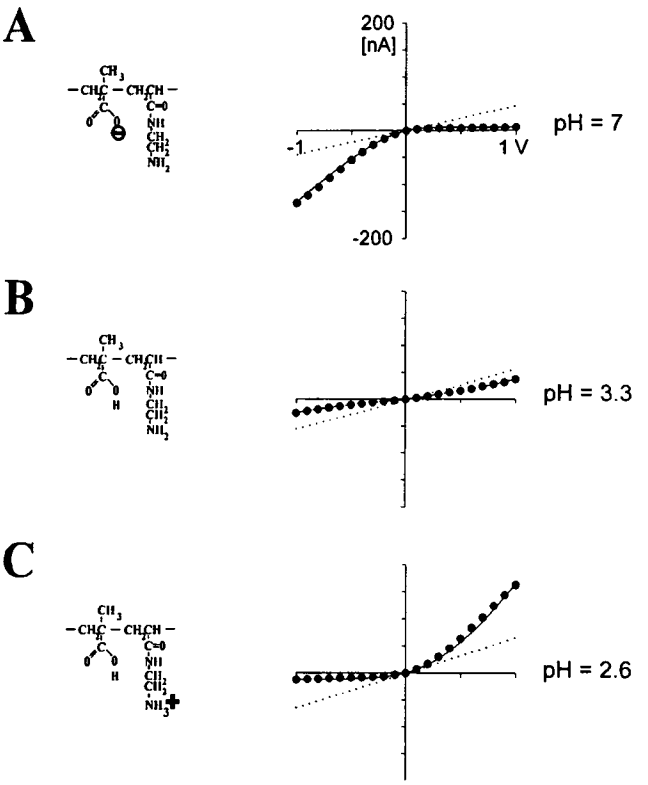

FIGURE 5 Current-voltage relationship (I-V) for synthetic amphoteric hydrogels. The charge characteristics of the monomeric repeating unit are shown in the left panel. The saline solution was composed of 10 mM KCl buffered at (*A*) pH 7.0 with Tris; (*B*) pH 3.3 with citric acid; and (*C*) pH 2.6 with citric acid. The pH of the solution inside and outside of the pipette was identical. Dotted lines represent the current-voltage relationship of the pipette in the absence of the gel particle (control current).

amplifies the current approximately threefold (compare curve with control), and at positive potentials it significantly reduces the current. This amplification and rectification of the current are very similar to that observed when the natural anionic hydrogel was attached to the pipette tip (Fig. 3 *A*; Nanavati and Fernandez, 1993). At pH 2.6 the synthetic gel has a net positive charge (Fig. 5 *C*) and, as expected, the gel rectified with a voltage dependence opposite that observed when the gel was negatively charged (Fig. 5 *A*). Amplification was also observed at positive potentials, with the current increasing ~threefold (compare I-V curve with control, Fig. 5 *C*). The solid lines in Fig. 5 *A* and *C* are the fits of Eq. 6 to the experimental data. The gel resistance (R_g) and the accumulation charge (z_{acc}) calculated from the fit at pH 2.6 (Fig. 5 *C*) are 3 MΩ and +0.13, respectively. The values obtained at pH 7 (Fig. 5 *A*) on a different particle are 5 MΩ and −0.18. The reason for the lower resistance at pH 2.6 is a result of the intrinsic variation among gels, the reduction in particle size, and the change in the number and nature of the fixed charges and counter-ions.

At pH 3.3, the synthetic microgel is neutral. Under these ionic conditions, no rectification was observed and the current-voltage relationship is approximately linear (Fig. 5 *B*). In addition, the current flowing was found to decrease ~twofold (compare curve with control, Fig. 5 *B*). Under these ionic conditions the gel resistance increased 3 to 5 times more than that observed when the gel was charged. This observation reinforces our hypothesis that the fixed charges of the gel are responsible for controlling the magnitude and direction of the current within the gel-pipette assembly. To further verify this conclusion we examined a synthetic gel that did not have ionizable groups. Outlined in Fig. 6 is the current-voltage relationship obtained when this gel was placed at the tip of a pipette (Fig. 1). For comparison, the current-voltage relationship of the anionic synthetic gel is also shown. As expected, the neutral gel did not rectify or amplify the current.

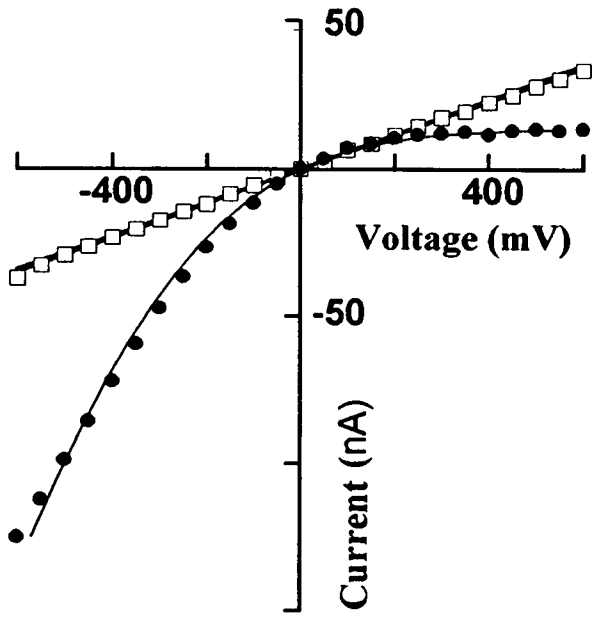

FIGURE 6 Steady-state current-voltage relationships for the anionic (●) and neutral (□) synthetic hydrogel microspheres. The solid line that crosses the filled circles is a fit of Eq. 6 to the experimental data. The saline in this experiment was composed of 20 mM NaCl and 5 mM TRIS, pH 6.9.

Pulsed laser imaging of ionic gradients

To further confirm the proposed mechanism of rectification and amplification of the current by the gel we used pulsed laser fluorescence microscopy (Kinosita et al., 1988; Monck et al., 1994). We used fluorescein as the ionic probe. In the absence of an applied voltage, anionic fluorescein is distributed homogeneously in solution but rearranges in the presence of an electric field. Thus it can be used to monitor local changes in ion concentrations at the gel-electrolyte interface.

Shown in Fig. 7 are snapshots of the fluorescent images captured when a 5-ms pulse of −9 V (left) or +9 V (right) was applied to the pipette with a natural gel attached. The bands of increasing fluorescence intensity indicate that there is an accumulation of ions at the gel-pipette solution interface during the application of a negative potential (bottom left). This accumulation of ions is accompanied by an increase in the current (top left). The images captured by firing the pulsed laser at various times after the onset of a +9 V pulse indicate that the depletion of the charge carriers from the gel-electrolyte interface occurs in milliseconds (Fig. 7, right). Notice that this depletion is directly correlated with the twofold decrease in the current at 5 ms (top right).

Although the images captured at 3 and 5 ms after the onset of the −9 V pulse (Fig. 7, left) indicate a threefold increase in fluorescence intensity, the actual maximal recorded intensity is sixfold. We present the images in this intensity range only to show the accumulation of charges present after 1 ms. Eq. 7 predicts a ~ 30-fold increase in concentration, which results in a fivefold difference from the experimental value. However, a quantitative comparison of the theory with these measurements is not currently possible because it requires a solution of the Nernst-Planck equation under non-steady-state conditions (c.f. Eq. 7). In addition, refinement of the experimental technique requires assessing the effects of several artifacts that decrease the fluorescence intensity. They include (i) the concentration dependent quenching of fluorescein and photobleaching of the dye, (ii) the out-of-focus light at the interface, and (iii) electroosmotic flow of the medium, particularly at high negative voltages. Despite these shortcomings the results shown in this section support the view that a focused electric field causes a rapid (ms) accumulation or depletion of ions at the interface between a charged hydrogel and an electrolyte. This accumulation and depletion of ions is directly correlated with the amplification and/or rectification of the measured current.

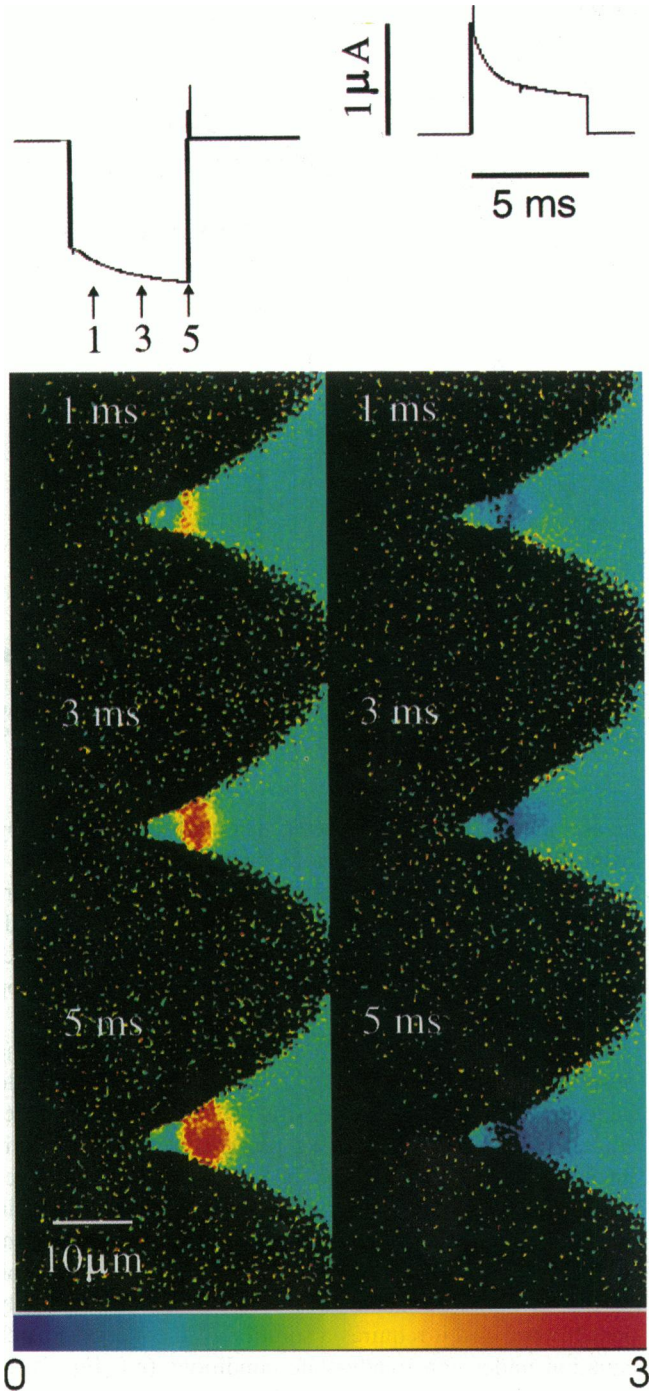

FIGURE 7 Pulsed laser imaging snapshots of the distribution of anionic fluorescein at the hydrogel-solution interface (natural hydrogel). The analog traces represent the current flowing through the particle in response to a 5-ms voltage pulse of −9 V (left) and +9 V (right). The arrows marked in the current trace correspond to the time at which the laser pulses were fired and the images captured. The orientation of the pipette and the localization of the granule gel are the same as outlined in Fig. 1 *B*, except that pipette P_2 was replaced by the reference electrode. The color bar represents the linear gradation in fluorescence intensity (0, low; 3, high). In these experiments the external saline solution was 15 mM histamine dihydrochloride and 10 mM HEPES, at a pH of 7.3. The solution in the pipette was the same except for the addition of 100 μM fluorescein

Fig. 8 shows three sets of pulsed laser images for three different types of gels: a natural anionic gel (top), a synthetic anionic gel (middle), and a neutral synthetic gel (bottom). These images were captured by firing the laser at the end of the pulse of a negative voltage (left arrow), and then at various times after the onset of the positive voltage. The internal gel-electrolyte interface is only visible in the images obtained with the charged gels (Fig. 8 *A* and *B*, natural and synthetic). Under a negative voltage, the anionic dye did not penetrate the highly charged natural gel (Fig. 8 *A*, 0 ms), but accumulated very quickly at the internal gel-electrolyte interface (analogous to Fig. 7, left). This accumulation of dye represents an increase in concentration of charge carriers that are responsible for the corresponding increase in the measured current. When the voltage reversed polarity, the accumulated ions were pushed out of the gel-electrolyte interface by electrophoresis (Fig. 8 *A*, 2 ms, observe the migrating band in the 2- and 5- ms snapshots) and the gel-electrolyte interface became depleted of charge carriers. This depletion of ions also parallels the decay of the measured ionic current.

The dye was able to penetrate the synthetic gel to some extent at negative potentials (Fig. 8, middle; the image was obtained 1 ms before the end of the first voltage pulse), but when the polarity of the voltage was reversed the dye split apart at the internal gel-electrolyte interface. The dye that penetrated the gel diffused into the surrounding medium, and the dye that accumulated at the interface was pushed by electrophoresis into the interior of the pipette. The images obtained for the neutral synthetic gel (bottom) show that this gel is easily penetrated by the anionic dye at negative potentials. In addition, there is no evidence of voltage-induced ionic gradients at the gel-electrolyte interface when the polarity was reversed. These observations correlate with the analog trace of the current in the leftmost lower panel in Fig. 8, and with the current-voltage relationship for the neutral gel in Fig. 6.

Relevance to biological systems

In nature, a charged polymer is often found adjacent to a pore in a cellular membrane. Some insight into how such biological interfaces might function can be construed from the results of this study. For example, during exocytosis a fusion pore joins the membrane of the secretory granule with the membrane of the cell. At this fusion pore the charged gel of the secretory granule is exposed to the extracellular electrolyte (Monck and Fernandez, 1994) and transient currents flow through this pore when the granule membrane potential is discharging (Breckenridge and Almers, 1987). In addition, the transient electric field within the fusion pore can induce ionic gradients at this junction. Outlined in Fig. 9 is a schematic showing the hypothetical distribution of ions in the fusion pore under the influence of potential gradients. There may be an accumulation (top) or depletion (bottom) of ions in the

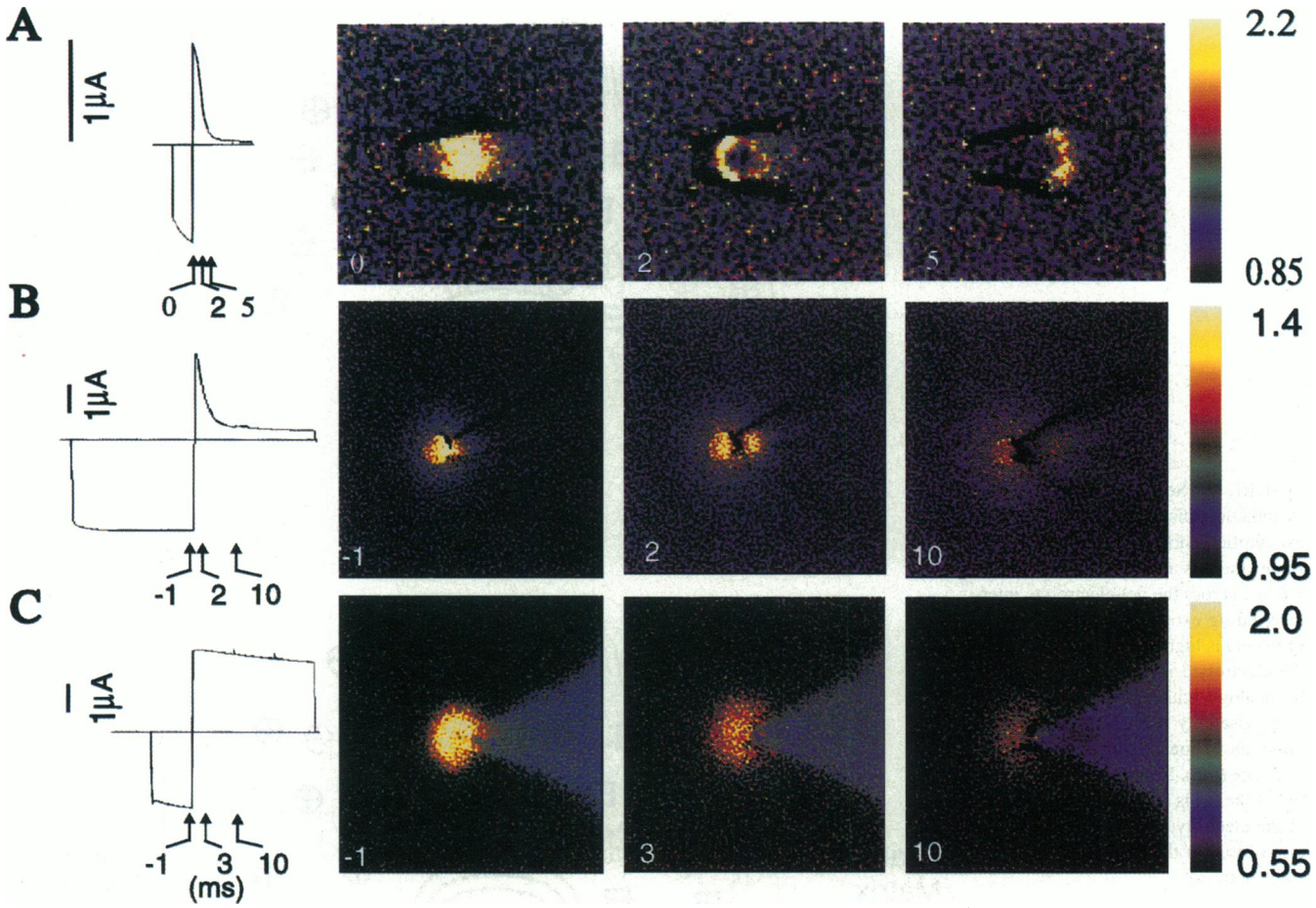

FIGURE 8 Pulsed laser imaging snapshots of the distribution of fluorescein near the interface of a gel exposed to a double voltage pulse. The outline of the pipettes is clearly visible in all images. Natural anionic gel microparticle (*A*); a charged synthetic gel microsphere (*B*), a neutral synthetic gel microsphere (*C*). The analog traces shown in the leftmost panels represent the currents through the gel-micropipette assembly in response to a negative voltage pulse followed immediately by a positive voltage pulse. The solution in the pipette contained 15 mM histamine dihydrochloride, 1 mM MES (pH 6), 100 μM fluorescein (*A*); 50 mM $CaCl_2$, 10 mM Tris (pH 7.5), 100 μM fluorescein (*B*). (*C*) The same as (*B*), except that the fluorescein concentration was 300 μM.

fusion pore at the granule-electrolyte interface. Because there is growing evidence to suggest that secretion occurs by ion exchange (Uvnäs and Åborg, 1989), any depletion or accumulation of ions at the fusion pore must influence this ion exchange and hence secretion. Although the diameter of the fusion pore (nanometer range) and the diameter of pipette tip (micron) are not the same, this difference is not critical, because the voltage ($\varphi^{sat} \cong -RT/(z_{acc}F)$ that causes the current to saturate (reverse current) is within the physiological range in the gel-pipette assembly (Fig. 3 *A*).

Other examples of rectifying interfaces are the interface between an ion channel and the intracellular cytoskeletal gel matrix (negatively charged) or an ion channel and extracellular polymeric structures (e.g., basement membrane bacterial or plant cell wall) (Paulsson et al., 1986; Delcour et al., 1992). In addition, the properties of the micron-sized hydrogel-electrolyte interfaces demonstrated here can be used to design miniature ionic devices that function in a wet environment (Cammak, 1992; Kajiwara and Ross-Murphy, 1992; Kishi and Osada, 1989; Kwon et al., 1991; Osada et al., 1992; Sucheta et al., 1992; Tanaka et al., 1982). Such devices may become the basis for "wet" integrated circuits executing and controlling electrochemical and biochemical reactions.

CONCLUSIONS

In an earlier paper Nanavati and Fernandez (1993) demonstrated that the secretory granule matrix rectifies and amplifies ionic currents when the granule is attached to a micropipette. In this study we show that these properties are caused by focusing an electric field at the interface between a charged gel and an electrolyte solution, which creates a voltage-dependent accumulation or depletion of ions. We suggest that similar ionic gradients might form during exocytosis and could control ion exchange at the fusion pore

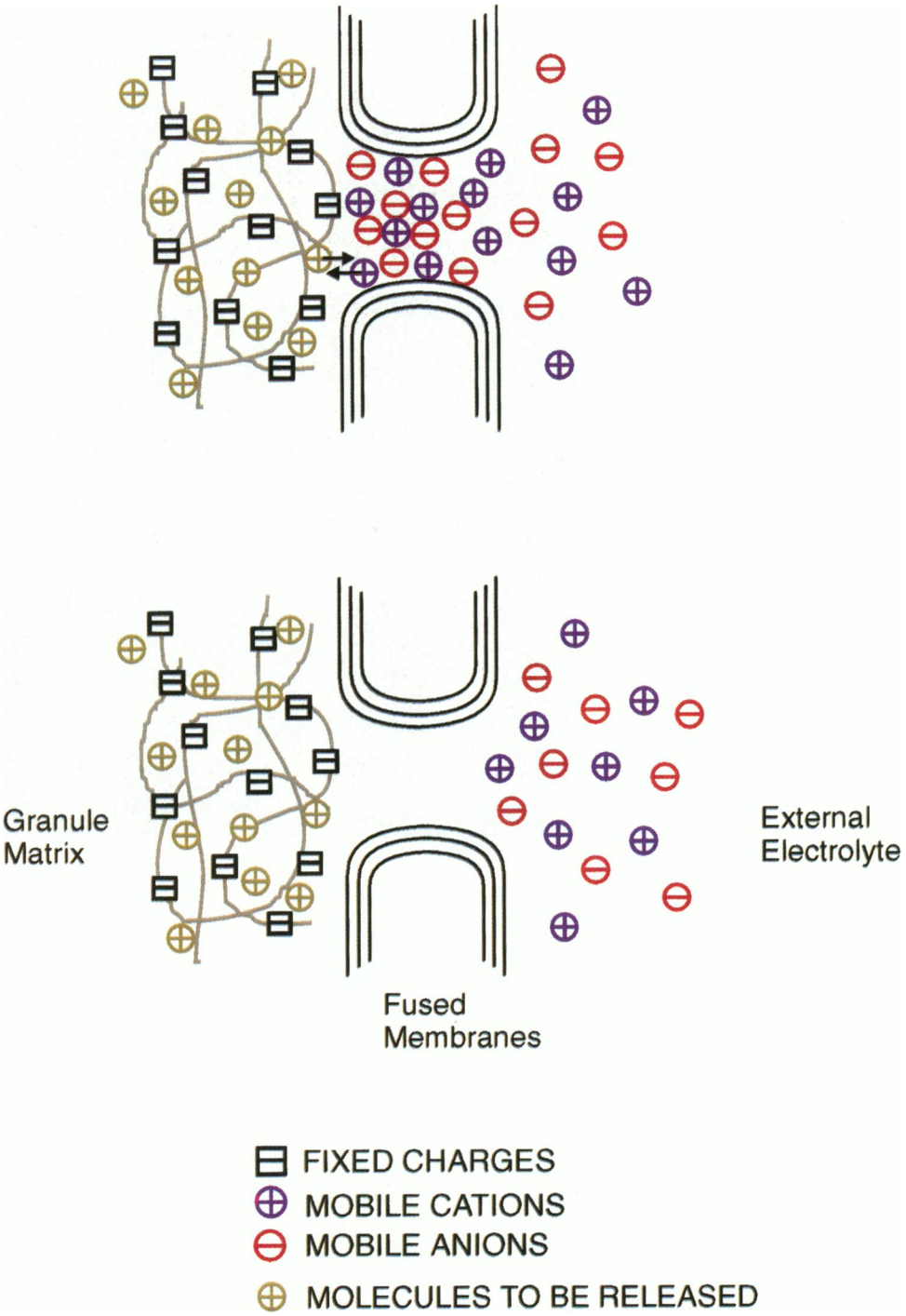

FIGURE 9 Schematic showing the hypothetical distribution of ions at the exocytotic fusion pore. This model assumes there is a transient potential difference across the gel-electrolyte interface during exocytosis. If the potential of the gel is higher than the potential of the electrolyte in the fusion pore then by analogy with the granule-micropipette assembly there will be an accumulation of ions at the gel-electrolyte interface (top). In contrast, if the potential of the gel is lower than the potential of the electrolyte there will be a depletion of ions at the gel-electrolyte interface (bottom).

and propose that the electrical properties of the secretory granule matrix should be considered when studying and/or modeling exocytotic events. In addition, by the use of pulsed-laser fluorescent microscopy we show for the first time the rapid formation of ionic gradients at a gel-electrolyte interface. This was possible because pulsed-laser imaging measures ionic distributions directly and with microsecond resolution and should be ideal for examining transient changes in ionic concentrations at other biological interfaces.

APPENDIX: DERIVATION OF THE CURRENT-VOLTAGE RELATIONSHIP FOR A CHARGED HYDROGEL MICROPARTICLE PLACED AT THE TIP OF A GLASS PIPETTE

The following expressions are derived for a spherical hydrogel attached to a glass pipette with conical shape. Spherical geometry provides a simple and convenient system of coordinates, however, neither the shape of the gel nor the shape of the electrode is critical for the rectification of ionic currents provided the electric field is focused at one and dispersed at a second gel-electrolyte interface.

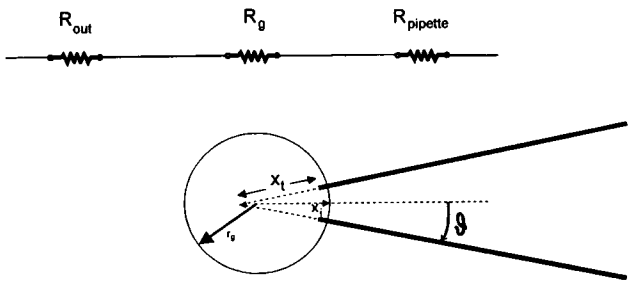

FIGURE A1 Schematic of the gel particle-micropipette assembly used to model the electrical phenomena at the gel-electrolyte interface. The resistance of the assembly is a sum of the resistance of the external medium, R_{out}, the resistance of the gel particle, R_g, and the resistance of the medium confined in the pipette, R_p (top). The hydrogel particle is modeled as a sphere of radius r_g. The pipette is modeled as a cone with an included angle, 2θ, which is truncated at its tip by a sphere of radius x_t. Spherical coordinates are used to describe the system. The surface of a gel particle in this coordinate system (the internal gel-electrolyte interface) has the coordinate x_i.

Resistance

Outlined in Fig. A1 is a schematic of the system used to model rectification of ionic currents by a hydrogel particle. We assume that the hydrogel is spherical with radius r_g and the pipette is a cone truncated at its tip by a sphere of radius x_t. The included angle of the cone is 2θ. In this assembly the gel is attached to the tip of the pipette.

We use spherical coordinates that are centered at the cone vortex. The coordinate of the internal gel-electrolyte interface is defined as x_i. The solid angle subtended by the pipette (ω_{in}) and the solid angle outside the pipette (ω_{out}) are given by

$$\omega_{in} = 2\pi(1 - \cos\theta) \tag{A1}$$

$$\omega_{out} = 2\pi(1 + \cos\theta) \tag{A2}$$

The total resistance of the system is the sum of the resistances of the external medium, R_{out}, the gel particle, R_g, and the medium confined in the pipette, R_p (Fig. A1, top), where R_{out} and R_p include the resistance of the external and internal gel-electrolyte interface, respectively. When the resistances are voltage independent the total resistance ($R = R^o$) is given by

$$R^0 = R^0_{out} + R^0_g + R^0_p \tag{A3}$$

The resistance of the medium in the pipette (R^0_p) and the external medium (R^0_{out}) is given by

$$R^0_p = \frac{\rho}{\omega_{in} x_i} \quad \text{and} \quad R^0_{out} = \frac{\rho}{\omega_{out} r_g} \tag{A4}$$

where ρ is the specific resistance of the saline. R^0_{out} was derived assuming the center of the gel coincides with the vortex of the cone.

Because the conical angle (θ) of the pipettes is $\sim 10°$ the solid angle outside the pipette is two orders of magnitude larger than the solid angle subtended by the pipette ($R^0_p/R^0_{out} \cong \omega_{out}/\omega_{in} = 131$). Therefore the resistance of the external solution around the micropipette contributes only about 1% to the total resistance of the system and may be neglected in the calculation of the current-voltage characteristics of the system.

Accumulation and depletion of ions at a gel-electrolyte interface

In this derivation we assume a steady state (independent of time) and neglect fluid convection in the pipette. We define the current flowing from the pipette toward the gel as positive. To simplify the derivation we assume that the solution only contains one binary electrolyte. The partial current densities i_+, i_- are given by the Nernst-Planck electrodiffusion equation:

$$i_k = z_k D_k F\left(\frac{dc_k}{dx} + \frac{F}{RT} z_k c_k \frac{d\varphi}{dx}\right) \tag{A5}$$

where φ is the electric potential, z is the ion charge number (valence), D is the diffusion coefficient, R is the gas constant, F is the Faraday constant, and the subscript k represents either cations or anions.

Electroneutrality requires that

$$z_+c_+ + z_-c_- = 0 \tag{A6}$$

The total current (I) flowing through any spherical cross section of the pipette at a distance x from the cone vortex is equal to

$$I = \omega_{in} x^2 (i_+ + i_-) \tag{A7}$$

In the absence of a gel there are no electrolyte gradients in the pipette, $dc_k/dx = 0$, and the resistance of the medium in the pipette can be obtained from Eqs. A5, A6 and A7:

$$R^0_p = \frac{RT}{F^2} \frac{1}{z_+ c^0_+ (z_+D_+ - z_-D_-)\omega x_i} \tag{A8}$$

where c^0_+ represents the concentration of cations in the absence of a gel. The fraction of current carried by cations (α_+) and anions (α_-) (transference numbers) is defined as

$$\alpha_+ = \frac{i_+}{i_+ + i_-} \quad \text{and} \quad \alpha_- = \frac{i_-}{i_+ + i_-} \tag{A9}$$

where, of course, $\alpha_+ + \alpha_- = 1$.

In addition, when there is no gel present the fraction of current carried by cations (α^0_+) and anions (α^0_-) satisfies the following equation:

$$\alpha^0_+ z_-D_- + \alpha^0_- z_+D_+ = 0 \tag{A10}$$

In the presence of a charged hydrogel, the transference numbers are determined by the properties of the hydrogel, i.e., by the concentrations and mobilities of its free (mobile) carriers. At the interface between the particle and the pipette solution the current densities are given by

$$i_+ = \alpha_+ \frac{I}{\omega x_i^2} \quad \text{and} \quad i_- = \alpha_- \frac{I}{\omega x_i^2} \tag{A11}$$

The concentration of electrolyte in the bulk solution (external or internal) is given by $c(\infty) = c^0$, $c_+(\infty) = c^0_+$, and $c_-(\infty) = c^0_-$. The concentration of electrolyte inside the pipette [$c(\infty)$] corresponds to the electric potential within the pipette [$\varphi(\infty) = \varphi_p$]. This potential is equal to the voltage applied to the electrode.

To obtain the ionic distribution within the pipette, the Nernst-Planck equations

$$i_+ = \alpha_+ \frac{I}{\omega x^2} = z_+D_+F \frac{dc_+}{dx} + \frac{F^2}{RT} z_+^2 D_+c_+ \frac{d\varphi}{dx} \tag{A12}$$

$$i_- = \alpha_- \frac{I}{\omega x^2} = z_-D_-F \frac{dc_-}{dx} + \frac{F^2}{RT} z_-^2 D_-c_- \frac{d\varphi}{dx} \tag{A13}$$

are solved for the condition of steady state.

Expressing A13 as the potential gradient,

$$\frac{d\varphi}{dx} = \frac{RT}{F^2 z_-^2 D_- c_-} \left(\alpha_- \frac{I}{\omega x^2} - z_-D_-F \frac{dc_-}{dx}\right) \tag{A14}$$

and substituting A14 into A12 and using the electroneutrality condition (A6), we derive the integral expression

$$\int_x^\infty \frac{dx}{x^2} = \frac{\omega F D_+}{I} \frac{z_+z_- - z_+^2}{z_-\left(\alpha_+ + \frac{\alpha_- z_+ D_+}{z_- D_-}\right)} \int_c^{c_0} dc_+ \qquad \text{(A15)}$$

After integrating from the gel-electrolyte interface to infinity we find an expression for the concentration of cations in the pipette:

$$c_+(x) = c_+^0 + z_- \frac{\alpha_+ z_- D_- + \alpha_- z_+ D_+}{z_+ z_- D_+ D_- (z_+ - z_-)} \frac{I}{F\omega} \frac{1}{x} \qquad \text{(A16)}$$

Likewise the distribution of anions is determined by

$$c_-(x) = -z_+ c_+(x)/z_-$$

To determine the distribution of the potential in the pipette first the ionic gradient (dc/dx) is determined from Eq. A16. This derivative is then expressed in terms of the total current (I), which is then substituted into A14. After further rearrangement $d\varphi$ is given by

$$d\varphi = -\frac{RT}{F} \frac{1}{\left[\frac{\alpha_+ z_- D_-}{D_- \alpha_+} + \frac{\alpha_- z_+ D_+}{D_+ \alpha_-}\right]} \frac{dc_-(x)}{c_-(x)} \qquad \text{(A17)}$$

We define the expression in brackets as the accumulation charge (z_{acc}):

$$z_{acc} = -\frac{\alpha_+ z_- D_- + \alpha_- z_+ D_+}{D_- \alpha_+ + D_+ \alpha_-} \qquad \text{(A18)}$$

Substituting A18 into A17 and replacing c with cz_+ and then integrating leads to the following expression:

$$\varphi(x) = \varphi_p - \frac{RT}{z_{acc} F} \ln\left[\frac{c(x)}{c^0}\right] \qquad \text{(A19)}$$

From A19 an expression for the electrolyte concentration at the internal gel-electrolyte interface is derived:

$$c(x_i) = c^0 \exp\left[\frac{z_{acc} F(\varphi_P - \varphi(x_i))}{RT}\right] \qquad \text{(A20)}$$

Current-voltage relationship for the gel-pipette assembly

A general expression for the current-voltage relationship of the system is derived by combining Eqs. A16 and A20:

$$I = F\omega x_i \frac{z_+ z_- D_+ D_- (z_+ - z_-)}{z_-(\alpha_+ z_- D_- + \alpha_- z_+ D_+)} \cdot c_+^0 \left\{\exp\left[\frac{z_{acc} F(\varphi_P - \varphi(x_i))}{RT}\right] - 1\right\} \qquad \text{(A21)}$$

where $\varphi_p - \varphi(x_i)$ is the potential drop in the pipette.

At low potentials this current-voltage expression is approximately linear and can be simplified to

$$I = \left\{\frac{z_{acc} F^2 \omega x_i c_+^0}{RT} \frac{z_+ D_+ D_- (z_+ - z_-)}{(\alpha_+ z_- D_- + \alpha_- z_+ D_+)}\right\} [\varphi_P - \varphi(x_i)] \qquad \text{(A22)}$$

where the expression in the curly brackets is the conductance $(R_p)^{-1}$ of the solution in the pipette at low potentials.

Dividing R_p by R_p^0 (Eq. A8), the ratio at low voltages is

$$\frac{R_p}{R_p^0} = \frac{(\alpha_+ D_- + \alpha_- D_+)(z_+ D_+ - z_- D_-)}{D_- D_+ (z_+ - z_-)} \qquad \text{(A23)}$$

Assuming $D_+ \cong D_-$, we can express Eq. A23 as

$$\frac{R_p}{R_p^0} = \frac{D_- D_+ (\alpha_+ + \alpha_-)(z_+ - z_-)}{D_- D_+ (z_+ - z_-)} \cong \alpha_+ + \alpha_- = 1 \qquad \text{(A24)}$$

Therefore at low voltages the resistance in the presence of the gel is close to the pipette resistance without the gel. Thus the current-voltage relationship for the assembly in the presence of the gel can be expressed as

$$I = -\frac{RT}{z_{acc} F} \frac{1}{R_p^0} \left\{1 - \exp\left[\frac{z_{acc} F(\varphi_p - \varphi(x_i))}{RT}\right]\right\} \qquad \text{(A25)}$$

Because the voltage drop across the external solution is small it can be neglected (see section on Resistance). Therefore we can express $\varphi(x_i)$ in terms of the voltage drop across the gel, i.e., $R_g I$. Thus the pipette potential can be expressed as

$$\varphi_p = R_g I + \frac{RT}{z_{acc} F} \ln\left[1 + \frac{z_{acc} F R_p^0}{RT} I\right] \qquad \text{(A26)}$$

This derivation is not only useful for the conical geometry outlined but is applicable to systems where the electric field is focused at a single gel-electrolyte interface (e.g., a cubic gel attached to a short uniform tube). Obviously this approach would yield different potential function and electrolyte concentrations with distance (cf. A16 and A19), but the current-voltage relationship would be analogous to A26 with the same z_{acc}.

We would like to thank Brenda Farrell for helpful discussion and for suggestions on the writing of the manuscript. This work was supported by grants from the National Institutes of Health and Tacora Co. to J.M.F.

We acknowledge salary support for V.S.M. from the National Institutes of Health grant to A.J. Hudspeth and for P.E.M. from Tacora Co.

REFERENCES

Bockris, J. O'M., and Reddy, A. K. N. 1977. Modern Electrochemistry, Vol. 1. Plenum Publishing, New York. 394–399.

Breckenridge, L. J., and W. Almers. 1987. Currents through the fusion pore that forms during exocytosis. *Nature.* 328:814–817.

Cammak, R. 1992. Plug in a molecular diode. *Nature.* 356:288–289.

Delcour, A. H., J. Adler, C. Kung, and B. Martinac. 1992. Membrane-derived oligosaccharides (MDO's) promote closing of an *E. coli* porin channel. *FEBS Lett.* 304:216–220.

DeRossi, D., K. Kajiwara, Y. Osada, and A. Yamauchi, eds. 1991. Polymer Gels: Fundamentals and Biomedical Applications. Plenum Press, New York.

Fernandez, J. M., M. Villalon, and P. Verdugo. 1991. Reversible condensation of mast cell secretory products in vitro. *Biophys. J.* 59:1022–1027.

Helfferich, F. 1962. Ion Exchange. McGraw-Hill Book Company, New York.

Kajiwara, K., and S. B. Ross-Murphy. 1992. Synthetic gels on the move. *Nature.* 355:208–209.

Kashiwabara, M., Y. Kasuya, K. Fujimoto, and H. Kawaguchi. 1993. *Polym. Prepr. Jpn.* 42:4623–4625.

Kinosita, K., Jr., I. Ashikawa, M. Hibino, M. Shigemori, H. Yoshimura, H. Itoh, K. Nagayama, and A. Ikegami. 1988. Submicrosecond imaging under a pulsed-laser fluorescence microscope. *Proc. Soc. Photo-Optical Instrum. Engineering.* 909:271–277.

Kishi, R., and Y. Osada. 1989. Reversible volume change of microparticles in an electric field. *J. Chem. Soc. Faraday Trans. 1* 85:655–662.

Kittel, C. 1976. Introdution to Solid State Physics. John Willey and Sons, New York. 242.

Kwon, I. C., Y. H. Bae, and S. W. Kim. 1991. Electrically erodible polymer gel for controlled release of drugs. *Nature.* 354:291–293.

Monck, J. R., and J. M. Fernandez. 1994. The exocytotic fusion pore and neurotransmitter release. *Neuron.* 12:707–716.

Monck, J. R., A. F. Oberhauser, G. Alvarez de Toledo, and J. M. Fernandez. 1991. Is swelling of the secretory granule matrix the force that dilates the exocytotic fusion pore? *Biophys. J.* 59:39–47.

Monck, J. R., A. F. Oberhauser, T. J. Keating, and J. M. Fernandez. 1992. Thin-section ratiometric Ca^{2+} images obtained by optical sectioning of Fura-2 loaded mast cells. *J. Cell Biol.* 116:745–759.

Monck, J. R., I. M. Robinson, A. L. Escobar, J. L. Vergara, and J. M. Fernandez. 1994. Pulsed laser imaging of rapid Ca^{2+} gradients in excitable cells. *Biophys. J.* 67:505–514.

Nanavati, C., and J. M. Fernandez. 1993. The secretory granule matrix: a fast-acting smart polymer. *Science.* 259:963–965.

Nanavati, C., V. S. Markin, A. F. Oberhauser, and J. M. Fernandez. 1992. The exocytotic fusion pore modeled as a lipidic pore. *Biophys. J.* 63:1118–1132.

Onsager, L. 1934. Deviations from Ohm's law in weak electrolytes. *J. Chem. Phys.* 2:599–615.

Osada, Y., H. Okuzaki, and H. Hori. 1992. A polymer gel with electrically driven motility. *Nature.* 355:242–244.

Paulsson, M., S. Fujiwara, M. Dziadek, R. Timpl, G. Pejler, G. Backstrom, U. Lindahl, and J. Engel. 1986. Structure and function of basement membrane proteoglycans. *In* Functions of the Proteoglycans. D. Evered and J. Whelan, editors. John Wiley and Sons, Chichester. 189–203.

Steinberg, I. Z., A. Oplatka, and A. Katchalsky. 1966. Mechanochemical engines. *Nature.* 210:568–571.

Sucheta, A., B. A. C. Ackrell, B. Cochran, and F. A. Armstrong. 1992. Diode-like behaviour of a mitochondrial electron-transport enzyme. *Nature.* 356:361–362.

Tam, P. Y., and P. Verdugo. 1981. Control of mucus hydration as a Donnan equilibrium process. *Nature.* 292:340–342.

Tanaka, T. 1981. Gels. *Sci. Am.* 244:124–138.

Tanaka, T., I. Nishio, S-T. Sun, and S. Ueno-Nishio. 1982. Collapse of gels in an electric field. *Science.* 218:467–469.

Uvnäs, B., and C.-H. Åborg. 1989. Role of ion exchange in release of biogenic amines. *News Physiol. Sci.* 4:68–71.